JOURNAL OF SOLID STATE CHEMISTRY **130,** 20–27 (1997)
ARTICLE NO. SC967253

Structural Evolutions in the $Sr_{1-x}Ba_xZrSe_3$ Series

Louis J. Tranchitella, Bai-Hao Chen,* James C. Fettinger, and Bryan W. Eichhorn

*Center for Superconductivity Research, Department of Chemistry and Biochemistry, University of Maryland, College Park, Maryland 20742; and *Lamont-Doherty Earth Observatory of Columbia University, Palisades, New York 10964*

Received June 17, 1996; in revised form December 2, 1996; accepted December 3, 1996

Compounds in the $Sr_{1-x}Ba_xZrSe_3$ series, where $0 \leq x \leq 0.68$, were prepared from SrSe, BaSe, Zr, and Se in evacuated and sealed silica ampules, at temperatures between 900 and 950°C. An amorphous Zr–Se phase is competitively formed in the reaction thus synthesis mixtures require 20 and 40% mole excess of Zr and Se, respectively. The $Sr_{1-x}Ba_xZrSe_3$ compounds adopt the NH_4CdCl_3 structure type, containing columns of double edge-sharing $ZrSe_6$ octahedra linked by distorted (Sr, Ba)Se_9 tricapped trigonal prisms. For $0.68 < x < 1.0$, biphasic mixtures of $CsNiCl_3$- and NH_4CdCl_3-type compounds are obtained. The $x \approx 1.0$ phase is a commensurate mismatched chain compound of formula $Ba_{1.07}ZrSr_3$. The (Sr, Ba)Se_9 tricapped prisms show a marked decrease in bond distance anisotropy as the Ba^{2+} concentration increases in the $Sr_{1-x}Ba_xZrSe_3$ series. The structure of $SrZrSe_3$ was determined from Rietveld profile analysis of the powder X-ray diffraction data whereas $Sr_{0.74}Ba_{0.26}ZrSe_3$ and $Sr_{0.32}Ba_{0.68}ZrSe_3$ were structurally characterized from single crystal X-ray studies. Crystallographic data for: (293 K)—orthorhombic, space group *Pnma*, $a = 8.915(1)$, $b = 3.965(1)$, and $c = 14.514(2)$ Å, $V = 513.1(1)$ Å^3, $Z = 4$, $R = 5.39\%$, and $R_{wp} = 6.55\%$; $Sr_{0.74}Ba_{0.26}ZrSe_3$ (293 K)—orthorhombic, space group *Pnma*, $a = 8.9305(2)$, $b = 3.9796(13)$, and $c = 14.611(2)$ Å, $V = 519.3(2)$ Å^3, $Z = 4$, $R(F_0) = 3.04\%$, $wR(F_0^2) = 5.95\%$; $Sr_{0.32}Ba_{0.68}ZrSe_3$ (293 K)—orthorhombic, space group *Pnma*, $a = 8.9741(11)$, $b = 4.0065(4)$, and $c = 14.7868(12)$ Å, $V = 531.66(9)$ Å^3, $Z = 4$, $R(F_0) = 4.12\%$, $wR(F_0^2) = 9.94\%$. © 1997 Academic Press

INTRODUCTION

The AMQ_3 compounds, where A = alkaline earth, Eu, Pb, Sn; M = Ti, Zr, Hf; Q = S, Se, exhibit a diverse and interesting crystal chemistry in which the $CsNiCl_3$, $GdFeO_3$, and NH_4CdCl_3 structure types are the most common. Early synthetic and structural studies on the $ATiQ_3$ phases where A = Ba, Sr (1–3) revealed $CsNiCl_3$-type structures characterized by strings of $^1_\infty[MQ_{6/2}]$ face-sharing octahedra that form channels filled by 12-coordinate A^{2+} cations. Saeki and co-workers have recently reported that some of the $CsNiCl_3$-type compounds are nonstoichiometric and are much more complicated than originally proposed. Their studies showed these phases to be incommensurate having the general formula $A_{1+x}TiS_3$ where A = Ba, Sr; $0.05 < x < 0.22$ (4–7). In contrast, the AMS_3 compounds with A = Ca, Sr, Ba, Eu; M = Zr, Hf (1, 3, 8, 9) were shown to adopt the perovskite-type $GdFeO_3$ structure characterized by buckled 3-D corner-sharing MS_6 octahedra. When A = Pb, Sn the zirconium and hafnium sulfides adopt the NH_4CdCl_3 structure type (9–11) that is typified by double columns of edge-sharing MS_6 octahedra linked by A^{2+} cations. Interestingly, high pressure studies have shown that the $SrZrS_3$ perovskite converts to a NH_4CdCl_3 structure at 60 kbar and 1000°C (12).

The $AMSe_3$ phases where A = Ca, Sr, Ba; M = Zr, Hf are not as well studied as the previous systems and ambiguities still exist. For example, Aslanov reported $BaZrSe_3$ to have the hexagonal $CsNiCl_3$ structure type with $P6_3/mmc$ symmetry, $a = 7.188$ Å and $c = 6.025$ Å (2). We have recently shown that this compound is also nonstoichiometric with a formula $Ba_{1.07}ZrSe_3$ and is a remarkable member of the commensurate mismatched chain compounds (13). Aslanov also reported that the $AZrSe_3$ compounds where A = Ca, Sr, and Pb were inaccessible although one would expect the Sr phase to exist and adopt the NH_4CdCl_3 structure in analogy to $EuZrSe_3$ (14). We report here the syntheses and structural analyses of $SrZrSe_3$ and its barium substituted derivatives of formula $Sr_{1-x}Ba_xZrSe_3$, where $0 \leq x \leq 0.68$. In contrast to the $Ba_{1.07}ZrSe_3$ compound, these phases adopt the commensurate NH_4CdCl_3 structure type and show a major change in the anisotropy of the $(Sr_{1-x}Ba_x)Se_9$ coordination sphere as x increases in the series.

EXPERIMENTAL

Synthesis

$Sr_{1-x}Ba_xZrSe_3$ samples in the $0 \leq x \leq 0.95$ range were prepared from BaSe, SrSe, Zr, and Se (CERAC Inorganics) by using a 20 and 40% molar excess of Zr and Se, respectively. The starting materials were ground in an N_2 dry box

0022-4596/97 $25.00

and sealed in evacuated silica ampules. The $x = 0$ sample, $SrZrSe_3$, was heated at 800°C for 5 days and cooled to room temperature. The sample was then reground, pressed into a pellet, and sealed in an evacuated silica ampule. The ampule was refired at 900°C for 7 days yielding "single phase" (by XRD), black microcrystalline $SrZrSe_3$. The samples with $x > 0$ were fired at 950°C for 5 days and cooled to room temperature in 4 h yielding brownish-black crystalline powders with black shiny irregular block-like single crystals (ca. 0.01 mm edges, $\sim$ 5% of sample) and long black needles (ca. 2–5 mm long, $\sim$ 10% of sample).

Analysis

Energy dispersive X-ray analysis (EDX) was performed on a JEOL JXA-840 A electron probe microanalyzer.

$Sr_{0.74}Ba_{0.26}ZrSe_3$ and $Sr_{0.32}Ba_{0.68}ZrSe_3$ were analyzed for Sr and Ba content by flame atomic absorption spectrophotometry on a Perkin–Elmer 2380 spectrophotometer using $SrCl_2$ and $BaCl_2$ as standards. Analyses were performed on single crystal samples dissolved in dilute HNO_3 (2%).

Bond valence analyses were performed using the methods of Brese and O'Keeffe (15, 16). The bond valence of the mixed sites containing barium and strontium were determined by calculating the valence for Sr and Ba as if each element occupied the site independently and a subsequent weighting by multiplication of the relative occupancies.

Structural Determination[1]

$Sr_{0.74}Ba_{0.26}ZrSe_3$. A black colored crystal with dimensions $0.03 \times 0.01 \times 0.01$ mm was placed on the Enraf–Nonius CAD-4 diffractometer. The crystals' final cell parameters and crystal orientation matrix were determined from 25 reflections in the range $20.2^\circ < 2\theta < 41.8^\circ$; these constants were confirmed with axial photographs. Data were collected [Mo$K\alpha$] with $\omega/2\theta$ scans over the range $2.7^\circ < \theta < 25.0^\circ$ with a scan width of $(0.90 + 0.35 \tan\theta)^\circ$ and a variable scan speed of 2.06–3.30° min^{-1}. Two ψ-scan reflections were collected twice over the range $10.3^\circ < \theta < 20.9^\circ$. The absorption correction was applied with transmission factors ranging from 0.8903–0.9959, average correction 0.9480. Data were corrected for Lorentz and polarization factors and absorption and were reduced to observe structure-factor amplitudes using the program package NRCVAX (17). Systematic absences indicated the centrosymmetric space group *Pmnb* (a nonstandard setting of *Pnma*, No. 62) or the noncentrosymmetric space group $P2_1nb$ (a nonstandard setting of $Pna2_1$: No. 33). Intensity statistics clearly indicated the centric case. The cell and data were reoriented to reflect the standard centric space group *Pnma* and the structure was then successfully determined (SHELX) (18). Refinement of the model with SHELXL-93, F_0^2 and $\sigma(F_0^2)$, converged well and the relative amounts of Ba and Sr at position 0.4347, 1/4, 0.6767 were determined to be Ba : Sr, 0.26 : 0.74 based on a constrained refinement (summed site occupancy = 100%). The structure was refined to convergence $[\Delta/\sigma \le 0.001]$ with $R(F) = 3.72\%$, $wR(F^2) = 6.11\%$ and GOF = 1.138 for all 531 unique reflections [$R(F) = 3.04\%$, $wR(F^2) = 5.95\%$ for those 461 data with $F_0 > 4\sigma(F_0)$]. A final difference-Fourier map was featureless with $|\Delta\rho| \le 0.973$ eA^{-3} with 1.2 Å of the heavy atoms. An empirical correction for extinction was also applied to the data in the form $(F_c^2, \text{corr}) = k[1 + 0.001 * x * F_c^2 * \lambda^3/\sin(2\theta)]^{(-1/4)}$ where $k = 0.15184$ is the overall scale factor. The value determined for x was 0.0075(5).

$Sr_{0.32}Ba_{0.68}ZrSe_3$. A black colored crystal with dimensions $0.03 \times 0.01 \times 0.01$ mm was placed on the Enraf–Nonius CAD-4 diffractometer. The crystals' final cell parameters and crystal orientation matrix were determined from 25 reflections in the range $20.0^\circ < 2\theta < 49.8^\circ$; these constants were confirmed with axial photographs. Data were collected [Mo$K\alpha$] with $\omega/2\theta$ scans over the range $2.7^\circ < \theta < 27.5^\circ$ with a scan width of $(0.90 + 0.35 \tan\theta)^\circ$ and a variable scan speed of 2.35°–4.12° min^{-1}. Data were corrected for Lorentz and polarization factors (but not absorption) and reduced to F_0^2 and $\sigma(F_0^2)$ using the program CAD4PC (19). Systematic absences indicated the centrosymmetric space group *Pnma* (No. 62) as was found in a previous structure determination. The atom positions from the previous refinement of $Sr_{0.74}Ba_{0.26}ZrSe_3$ were used as the initial structural model. Refinement of the model with SHELXL-93 (18) on F_0^2 and $\sigma(F_0^2)$, converged well and the relative amounts of Ba and Sr at position 0.4327, 1/4, 0.6751, were determined to be Ba : Sr, 0.68 : 0.32 based on a constrained refinement (summed site occupancy = 100%). The structure was refined to convergence $[\Delta/\sigma \le 0.001]$ with $R(F) = 5.18\%$, $wR(F^2) = 10.40\%$ and GOF = 1.031 for all 531 unique reflections [$R(F) = 4.12\%$, $wR(F^2) = 9.94\%$ for those 582 data with $F_0 > 4\sigma(F_0)$]. A final difference-Fourier map revealed rather large peaks, $|\Delta\rho| \le 3.59$ eÅ^{-3} within 1.0 Å of the heavy atoms. An empirical correction for extinction was also applied to the data in the form $(F_c^2, \text{corr}) = k[1 + 0.001 * x * F_c^2 * \lambda^3/\sin(2\theta)]^{(-1/4)}$

[1] See NAPS document No. 05385 for 48 pages of supplementary material. This is not a multi-article document. Order from NAPS c/o Microfiche Publications, P.O. Box 3513, Grand Central Station, New York, NY 10163-3513. Remit in advance in U.S. funds only $16.15 for photocopies or $5.00 for microfiche. There is a $15.00 invoicing charge on all orders filled before payment. Outside U.S. and Canada add postage of $4.50 for the first 20 pages and $1.00 for each 10 pages of material thereafter, or $1.75 for the first microfiche and 50¢ for each microfiche thereafter.

where $k = 0.20210$ is the overall scale factor. The value determined for x was 0.036(2).

Powder X-ray Refinements

Powder X-ray diffraction (XRD) data for all samples were collected at 25°C on a modified Phillips XRG 2000 diffractometer (Cu$K\alpha$) interfaced with a RADIX databox and a MDI software system. Data were collected in the $20^\circ \leq 2\theta \leq 60^\circ$ range ($20^\circ \leq 2\theta \leq 70^\circ$ for $SrZrSe_3$). Data for $SrZrSe_3$ were collected with step widths of 0.02° and step times of 20.0 s. Cell refinement calculations were performed on all data and corrected for zero-point error. Rietveld profile analyses (Riqas, MDI) were conducted using split Pearson VII profile shape functions and initial atomic coordinates and cell constants taken from $EuZrSe_3$ (14) or the single crystal studies described above. Initial structural analysis involved the refinements of the structure factors, lattice parameters, zero point terms, background coefficients, and peak shape parameters. The positional parameters and isotropic thermal parameters for all atoms were refined in the latter cycles.

RESULTS

Synthesis and Structural Characterization

The $Sr_{1-x}Ba_xZrSe_3$ compounds where $0 \leq x \leq 0.68$ were prepared from SrSe, BaSe, Zr, and Se in the presence of 20% excess Zr and 40% excess Se. The precursors were fired for 5–7 days at 900–950°C in sealed silica ampules. The "pure phases" (by XRD) were only obtained with excess Zr and Se present in the synthesis mixtures presumably due to the competitive formation of an amorphous Zr–Se phase (see below). The samples are dark brownish-black microcrystalline powders with black shiny irregular block-like single crystals ($\leq 5\%$) and black needles ($\leq 10\%$) in some of the mixtures. The compounds were analyzed by EDX, atomic absorption, XRD, and single crystal X-ray diffraction. EDX analysis of the irregular blocks indicated Sr, Ba, Zr, and Se were all present (except for the $x = 0$ phase), while analysis of the needles showed only Zr and Se. Atomic absorption performed on irregular blocks of $Sr_{0.74}Ba_{0.26}ZrSe_3$ and $Sr_{0.32}Ba_{0.68}ZrSe_3$ revealed Sr-to-Ba ratios of $0.75 \pm 0.01 : 0.25 \pm 0.01$ for the former and $0.29 \pm 0.01 : 0.71 \pm 0.01$ for the latter. Both types of crystals were examined by single crystal X-ray diffraction. The needles did not diffract suggesting that an amorphous Zr–Se phase was formed that was not detected in the XRD analyses.

$Sr_{1-x}Ba_xZrSe_3$ compositions where $0.68 < x < 1.0$ give biphasic mixtures of products that appear to contain NH_4CdCl_3-type and $CsNiCl_3$-related compounds. Due to the poor crystallinity and numerous overlapping peaks in the XRD profiles, their compositions were not discernible. Compositions of formula $BaZrSe_3$ that were processed under identical conditions give the commensurate mismatched chain compound $Ba_{1.07}ZrSe_3$ (13) as the only identifiable species. Attempted crystallizations of "$BaZrSe_3$" using a $SrCl_2$ flux gave crystals of $Sr_{0.32}Ba_{0.68}ZrSe_3$ as determined by single crystal X-ray diffraction. Attempted preparations of $CaZrSe_3$ by similar methods yielded only CaSe and $ZrSe_2$.

The structure of $SrZrSe_3$ was successfully refined from powder X-ray diffraction data by Rietveld profile analysis. The profile fits of $SrZrSe_3$ and $Sr_{0.76}Ba_{0.24}ZrSe_3$ are shown in Fig. 1 and a summary of the refinement data for $SrZrSe_3$ is given in Table 1. The lattice constants for $Sr_{0.76}Ba_{0.24}ZrSe_3$ ($a = 8.935(3)$, $b = 3.981(1)$, and $c = 14.614(4)$ Å) and resulting atomic coordinates from the Rietveld analysis are essentially the same as the single crystal data for $Sr_{0.74}Ba_{0.26}ZrSe_3$ (see below), with very minor differences in the refined compositions. An unidentified impurity is present in both samples (darkened peaks, Figs. 1a and 1b) that probably represents ca. 5% of the samples. Two representative $Sr_{1-x}Ba_xZrSe_3$ compounds, the $x = 0.26$ and $x = 0.68$ members, were also characterized by single crystal X-ray diffraction. Crystals of the latter compound were obtained from a synthesis mixture containing a 0.25 : 0.75 Sr-to-Ba ratio. A summary of the single crystal data for these compounds is given in Table 2. Listings of fractional coordinates and selected bond distances and angles for the $x = 0$, 0.26, and 0.68 $Sr_{1-x}Ba_xZrSe_3$ compounds are given in Tables 3 and 4. A plot of lattice parameter versus composition is given in Fig. 2. As expected, as the larger Ba is substituted for Sr (IX coord. Ba^{2+}, $r_i = 1.47$ Å; IX coord. Sr^{2+}, $r_i = 1.31$ Å) (20) there is a quasi-linear increase of a, b, and c as x increases, however, the largest percentage increase (1.9%) is observed along the c axis.

Solid State Structures

The $Sr_{1-x}Ba_xZrSe_3$ compounds where $0 \leq x \leq 0.68$ adopt the NH_4CdCl_3 structure type with *Pnma* crystal symmetry and are isotypic with $EuZrSe_3$ (14). The structure contains double columns of edge-sharing $ZrSe_6$ octahedra running parallel to the b axis. The chains are linked by $(Sr, Ba)Se_9$ distorted tricapped trigonal prisms as shown in Fig. 3.

The $ZrSe_6$ chains are essentially identical in the three crystallographically characterized compounds described here as well as the $EuZrSe_3$ phase described by Mar and Ibers (14). The Zr–Se distances range from 2.544(7) to 2.779(6) Å with average Zr–Se distances of 2.68(1) Å ($x = 0$), 2.69(1) Å ($x = 0.26$), and 2.70(1) Å ($x = 0.68$). The corresponding bond valence analyses (16) yields Zr valencies of $+4.0$, $+3.9$, and $+4.0$, respectively. Significant changes

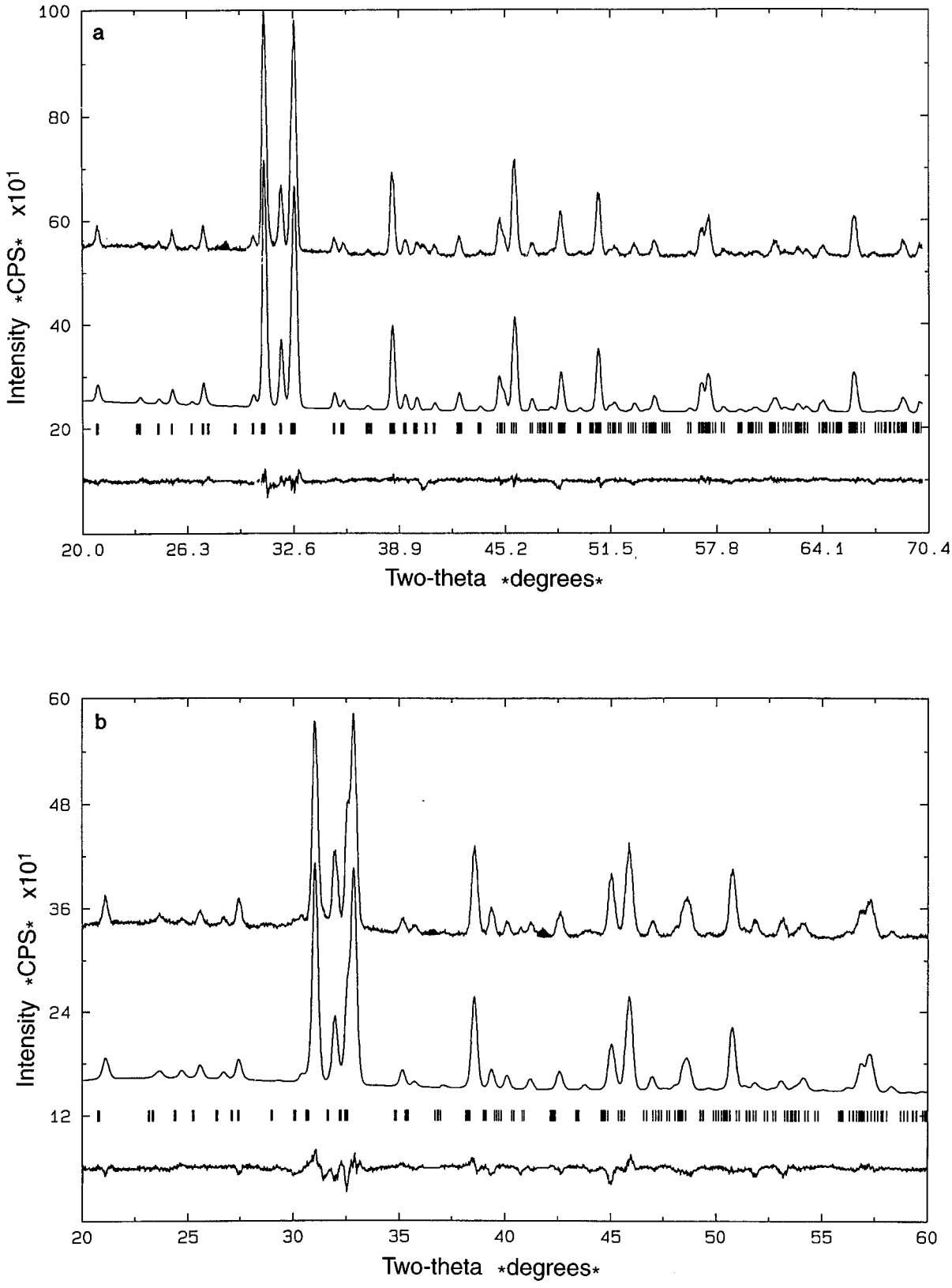

FIG. 1. The observed (top), calculated (middle), and difference (bottom) X-ray diffraction profiles from Rietveld Profile analyses of (a) $SrZrSe_3$ and (b) $Sr_{0.76}Ba_{0.24}ZrSe_3$.

TABLE 1
Summary of Crystallographic Data (Rietveld Profile Refinement) for $SrZrSe_3$

Formula	$SrZrSe_3$
Space group	*Pnma*
a(Å)	8.915(1)
b(Å)	3.965(1)
c(Å)	14.514(1)
V(Å^3)	513.1(1)
Z	4
ρ_{cal}(g/cm^3)	5.381(2)
R(%)	5.39
R_{wp}(%)	6.55
R_{Bragg}(%)	6.25

Note. $R = \{[\sum(P_0 - P_c)^2]/\sum(P_0)^2]\}^{1/2}$, $R_{wp} = \{[\sum w(P_0 - P_c)^2]/[\sum w(P_0)^2]\}^{1/2}$, and $R_{Bragg} = [\sum|F_0 - F_c|]/\sum(F_0)]$.

TABLE 3
Fractional Coordinates for the $Sr_{1-x}Ba_xZrSe_3$ Compounds[a] where $x = 0$, 0.24, 0.26, and 0.68

	$SrZrSe_3$		$Sr_{0.74}Ba_{0.26}ZrSe_3$		$Sr_{0.32}Ba_{0.68}ZrSe_3$	
	x	z	x	z	x	z
Sr/Ba	0.4404(5)	0.6792(3)	0.4347(1)	0.6767(1)	0.4327(1)	0.6751(1)
Zr	0.1720(5)	0.4416(3)	0.1684(1)	0.4419(1)	0.1657(1)	0.4408(1)
Se(1)	0.0195(6)	0.6086(3)	0.0223(1)	0.6074(1)	0.0254(1)	0.6067(1)
Se(2)	0.1637(6)	0.0128(3)	0.1620(1)	0.0107(1)	0.1645(1)	0.0073(1)
Se(3)	0.2886(5)	0.2816(4)	0.2907(1)	0.2828(1)	0.2887(1)	0.2843(1)

[a] For $SrZrSe_3$, $T = 293$ K (Rietveld profile analysis), for $Sr_{0.74}Ba_{0.26}ZrSe_3$, $T = 293$ K (single crystal), and for $Sr_{0.32}Ba_{0.68}ZrSe_3$, $T = 293$ K (single crystal).

in the Zr–Se distances are not expected since an isovalent substitution on the Sr site does not have a direct effect on the Zr–Se bonding.

In contrast, the (Sr, Ba)Se_9 distorted tricapped trigonal prisms show large changes in the (Sr, Ba)–Se distances and the anisotropy of the coordination sphere as x changes. In $SrZrSe_3$, the Sr^{2+} ions are pseudo-nine coordinate with eight Sr–Se distances ranging from 3.160(6) to 3.425(6) Å. An additional longer Sr–Se contact of 3.890(7) Å is observed which gives an average Sr–Se distance of 3.308(7) Å. As expected, the Sr–Se distances in the nine-coordinate environment of $SrZrSe_3$ are longer than the

TABLE 2
Summary of Crystallographic Data (Single Crystal) for $Sr_{0.74}Ba_{0.26}ZrSe_3$ and $Sr_{0.32}Ba_{0.68}ZrSe_3$

	$Sr_{0.74}Ba_{0.26}ZrSe_3$	$Sr_{0.32}Ba_{0.68}ZrSe_3$
Formula	$Sr_{0.74}Ba_{0.26}ZrSe_3$	$Sr_{0.32}Ba_{0.68}ZrSe_3$
Formula weight (amu)	428.89	449.40
Space group	*Pnma*	*Pnma*
a(Å)	8.931(1)	8.974(1)
b(Å)	3.980(1)	4.007(1)
c(Å)	14.611(2)	14.787(1)
β(°)	90	90
V(Å^3)	519.3(2)	531.7(1)
T(K)	293(2)	293(2)
Z	4	4
ρ_{cal} (g/cm^3)	5.486	5.614
No. of refln.	2005	1371
No. of unique refln.	531	699
No. unique refln. w/ $F_0 > 4\sigma F_0$	461	582
No. of variables	33	33
Radiation [Mo$K\alpha$] (Å)	0.71073	0.71073
μ (mm^{-1})	21.123	20.617
$R(F_0)$	3.04	4.12
$wR(F_0^2)$	5.95	9.94
G.O.F.	1.138	1.031

Note. For single crystal refinements, $R(F_0) = [\sum(F_0 - F_c)/\sum(F_0)]$ and $wR(F_0^2) = [\sum w(F_0^2 - F_c^2)/\sum w(F_0^2)]^{1/2}$.

TABLE 4
Selected Interatomic Distances (Å) and Bond Angles (°) for the $Sr_{1-x}Ba_xZrSe_3$ Compounds[a] where $x = 0$, 0.26, and 0.68

Bond	mult.	$x = 0$	$x = 0.26$	$x = 0.68$
Sr/Ba–Se(1)		3.160(6)	3.249(1)	3.332(1)
Sr/Ba–Se(1)		3.890(7)	3.819(1)	3.793(2)
Sr/Ba–Se(2)	2×	3.260(5)	3.254(1)	3.307(1)
Sr/Ba–Se(2)		3.4247(6)	3.409(1)	3.406(2)
Sr/Ba–Se(3)	2×	3.177(5)	3.213(1)	3.251(1)
Sr/Ba–Se(3)	2×	3.211(5)	3.226(1)	3.260(1)
Zr–Se(1)	2×	2.716(5)	2.716(1)	2.729(1)
Zr–Se(1)		2.779(6)	2.747(1)	2.758(2)
Zr–Se(2)	2×	2.673(4)	2.695(1)	2.702(1)
Zr–Se(3)		2.544(7)	2.570(1)	2.563(1)
Angle	**mult.**	**$x = 0$**	**$x = 0.26$**	**$x = 0.68$**
Se(1)–Zr–Se(1)	2×	85.78(4)	86.33(3)	86.67(4)
Se(1)–Zr–Se(1)		93.77(7)	94.19(5)	94.46(5)
Se(2)–Zr–Se(1)	2×	84.65(3)	84.87(3)	84.48(3)
Se(2)–Zr–Se(1)	2×	86.04(2)	86.48(4)	86.22(2)
Se(2)–Zr–Se(1)	2×	171.8(5)	172.80(5)	172.86(6)
Se(2)–Zr–Se(2)		95.76(6)	95.16(5)	95.70(6)
Se(3)–Zr–Se(1)	2×	90.96(5)	91.51(4)	92.19(4)
Se(3)–Zr–Se(1)		174.8(5)	176.83(5)	178.31(6)
Se(3)–Zr–Se(2)	2×	97.41(4)	95.65(4)	94.91(4)

[a] For $SrZrSe_3$, $T = 293$ K (Rietveld profile analysis), for $Sr_{0.74}Ba_{0.26}ZrSe_3$, $T = 293$ K (single crystal), and for $Sr_{0.32}Ba_{0.68}ZrSe_3$, $T = 293$ K (single crystal).

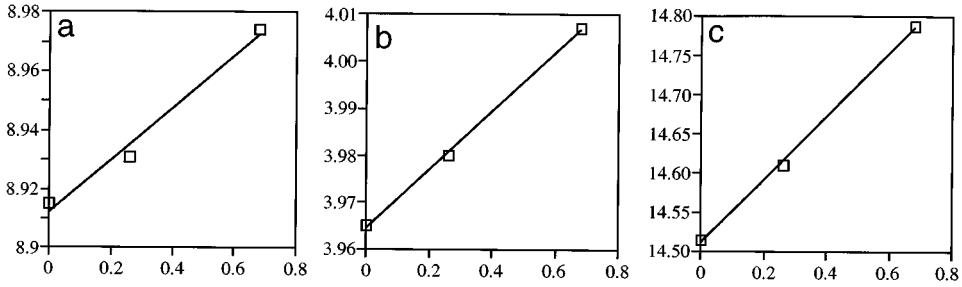

FIG. 2. Plot of lattice parameter (Å) versus x for compounds in $Sr_{1-x}Ba_xZrSe_3$ series.

six-coordinate Sr–Se contacts of 3.115 Å in SrSe (21). The average (Sr, Ba)–Se distances increase from 3.308(7) Å in $SrZrSe_3$ to 3.318(1) Å in $Sr_{0.74}Ba_{0.26}ZrSe_3$ to 3.352(1) Å in $Sr_{0.32}Ba_{0.68}ZrSe_3$. In addition, the (Sr, Ba)–Se distances become increasingly isotropic as more Ba is substituted onto the A site. For example, the differences in the (Sr, Ba)–Se contacts within a given compound decrease from 0.73 Å in $SrZrSe_3$ to 0.61 Å in $Sr_{0.74}Ba_{0.26}ZrSe_3$ to 0.54 Å in $Sr_{0.32}Ba_{0.68}ZrSe_3$. The longer (Sr, Ba)–Se distance *decreases* from 3.890(7) Å in $SrZrSe_3$ to 3.820(1) Å in $Sr_{0.74}Ba_{0.26}ZrSe_3$ to 3.793(2) Å in $Sr_{0.32}Ba_{0.68}ZrSe_3$ despite the larger average ionic radius at the A site. The increasingly isotropic nature of the Sr, Ba site is presumably due to the larger coordination sphere of barium relative to strontium. Figure 4 illustrates the differences in the (Sr, Ba)Se_9 polyhedra in the $SrZrSe_3$ and $Sr_{0.32}Ba_{0.68}ZeSe_3$ compounds. Bond valence analyses yielded valencies of $+1.5$, $+1.8$, and $+2.2$ for the A-site ions (weighted average) in $SrZrSe_3$, $Sr_{0.74}Ba_{0.26}ZrSe_3$, and $Sr_{0.32}Ba_{0.68}ZrSe_3$, respectively.

DISCUSSION

In an attempt to prepare ternary selenides with perovskite structures, we postulated that by lowering the pressure in a NH_4CdCl_3-type $AZrSe_3$ phase through isovalent A-site substitution, a perovskite-type selenide compound may be obtained. This behavior would be the reverse of the high pressure perovskite-to-NH_4CdCl_3-type structural transition observed in the $SrZrS_3$ system (12). Although this approach has not yielded any perovskites thus far, there are interesting structural transformations in the $Sr_{1-x}Ba_xZrSe_3$ system that provide insight into the stability ranges of the NH_4CdCl_3-type sulfides and selenides. In contrast to the original report by Aslanov, we have found that $SrZrSe_3$ does exist and adopts the commensurate NH_4CdCl_3 structure type as expected. Attempted preparations of the compound from stoichiometric synthesis mixtures gives complicated multiphase products which probably lead Aslanov to conclude that the phase was not accessible. We have found that the "single phase" compound can only be prepared in the presence of excess Zr and Se due to a competitive formation of an amorphous Zr–Se material. Likewise, the $Sr_{1-x}Ba_xZrSe_3$ phases where $0 \leq x \leq 0.68$ also require excess Zr and Se in their synthesis mixtures and also adopt the NH_4CdCl_3 structure. However, structural studies on the $Sr_{1-x}Ba_xZrSe_3$ phases show a marked decrease in the anisotropy of the (Sr, Ba)Se_9 coordination sphere as the Ba^{2+} concentration increases. For $SrZrSe_3$, Sr is probably best described as eight-coordinate whereas $Sr_{0.32}Ba_{0.68}ZrSe_3$ clearly has nine-coordinate (Sr, Ba)Se_9 sites. In contrast, the Zr–Se bonding remains essentially unchanged throughout the solid solution series. As the average size of the A-site cation increases in the $Sr_{1-x}Ba_xZrSe_3$ series, it appears that the NH_4CdCl_3 structure type becomes unstable with respect to the $CsNiCl_3$ structure. The decrease in anisotropy of the ASe_9 coordination sphere (i.e., the coordination number of A) does *not* seem to trigger the instability in that the NH_4CdCl_3 compound $LaCrSe_3$ has highly isotropic $LaSe_9$ polyhedra but with much shorter A–Se bond (La–Se bonds range from 3.07 to 3.25 Å) (22). More likely, the size constraints of the A-site "hole" in the $Sr_{1-x}Ba_xZrSe_3$ series cannot accommodate the large Ba^{2+} ion beyond 2/3 filling. The increase in the A-site bond valencies for the $Sr_{1-x}Ba_xZrSe_3$ series with increasing Ba^{2+} concentration ($+1.5 \rightarrow +2.2$) may signify this instability. However, these values are in "acceptable ranges" for sulfides and selenides in that bond valence analyses are not as accurate for these compounds relative to the more ionic oxides.

Aslanov also reported the initial synthesis of $BaZrSe_3$ which is characterized as a $CsNiCl_3$ compound. However, we have recently found this compound to be nonstoichiometric with a composition of $Ba_{1.07}ZrSe_3$ and is a remarkable member of the recently discovered $A_{1+x}MQ_3$ commensurate mismatched chain compounds (13). Our attempts to prepare stoichiometric $BaZrSe_3$ have been unsuccessful.

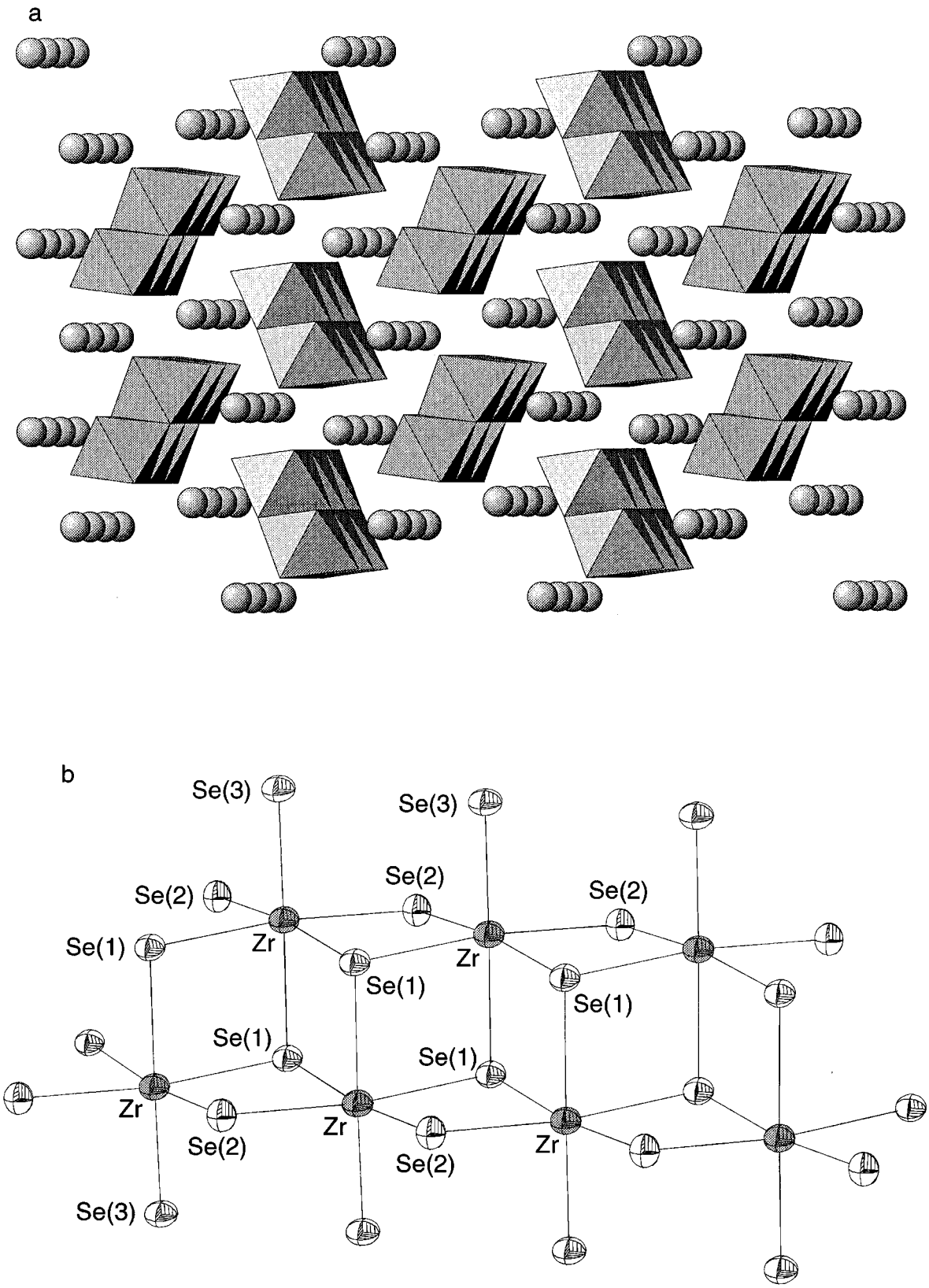

FIG. 3. (a) Polyhedral representation of $SrZrSe_3$. The shaded spheres represent the Sr^{2+} ions. (b) Ball and stick drawing showing the linked $ZrSe_6$ octahedra.

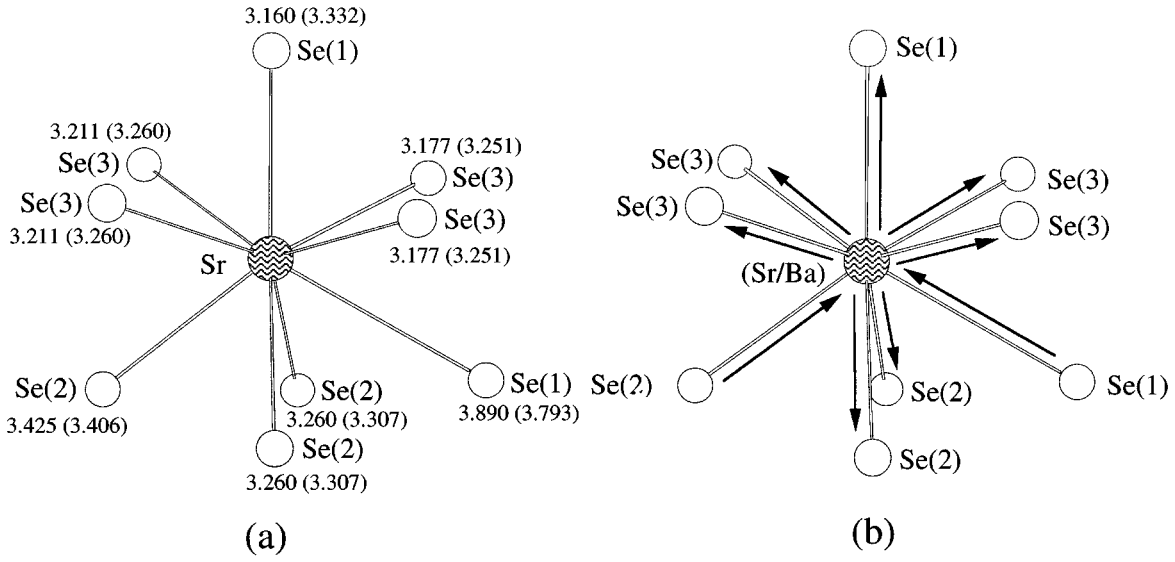

FIG. 4. (a) Ball and stick drawing of the $SrSe_9$ polyhedron in $SrZrSe_3$. The numbers denote M–Se bond distances for $SrZrSe_3$ and $Sr_{0.32}Ba_{0.68}ZrSe_3$ (in parentheses). (b) Ball and stick drawing of the $(Sr/Ba)Se_9$ polyhedron in $Sr_{0.32}Ba_{0.68}ZrSe_3$. The arrows depict direction of change in the (Sr/Ba)–Se bonds upon increasing Ba^{2+} concentration.

ACKNOWLEDGMENT

We thank Michelle Clarke and Jordan Adelson for their assistance in performing the flame atomic absorption studies. This work was funded by the NSF (DMR-9223060) and Electric Power Research Institute.

REFERENCES

1. H. Hahn and U. Mutschke, *Z. Anorg. Allg. Chem.* **288,** 269 (1956).
2. L. A. Aslanov, *Russ. J. Inor. Chem.* **9,** 1090 (1964).
3. A. Clearfield, *Acta Crystallogr.* **16,** 135 (1963).
4. M. Onoda and M. Saeki, *Jpn. J. Appl. Phys.* **32,** 752 (1993).
5. M. Onoda, M. Saeki, A. Yamamoto, and K. Kato, *Acta Crystallogr. B* **49,** 929 (1993).
6. M. Saeki and M. Onoda, *J. Solid State Chem.* **102,** 100 (1993).
7. M. Saeki and M. Onoda, *J. Solid State Chem.* **112,** 65 (1994).
8. L. A. Aslanov and M. Kovba, *Russ. J. Inor. Chem.* **9,** 1317 (1964).
9. R. Lelieveld and D. J. W. Ijdo, *Acta Crystallogr. B* **36,** 2223 (1980).
10. G. A. Wiegers, A. Meetsma, R. J. Haange, and J. L. DeBoer, *Acta Crystallogr. C* **45,** 847 (1989).
11. A. Meetsma, G. A. Wiegers, and J. L. DeBoer, *Acta Crystallogr. C* **49,** 2060 (1993).
12. B. Okai, K. Takahashi, M. Saeki, and J. Yoshimoto, *Mat. Res. Bull.* **23,** 1575 (1988).
13. L. Tranchitella, P. K. Dorhout, J. C. Fettinger, and B. W. Eichhorn, submitted for publication.
14. A. Mar and J. A. Ibers, *Acta. Crystallogr. C* **48,** 771 (1992).
15. M. O'Keeffe, *Acta Crystallogr. A* **46,** 138 (1990).
16. N. E. Brese and M. O'Keeffe, *Acta Crystallogr. B* **47,** 192 (1991).
17. E. J. Gabe, Y. L. Page, J.-P. Charland, F. Lee, and P. S. White, *J. Appl. Crystallogr.* **22,** 384 (1989).
18. G. M. Sheldrick, *Acta Crystallogr, A* **46,** 467 (1990).
19. K. Harms, "XCAD4 Data Processing Package," University of Marburg (1993).
20. R. D. Shannon, *Acta Crystallogr. A* **32,** 751 (1976).
21. M. K. Slattery, *Phys. Rev.* **25,** 333 (1925).
22. N. Huy-Dung, J. Etienne, and P. Laruelle, *Bull. Soc. Chim. Fr.*, 2433 (1971).